Establishment and formation of fog-dependent *Tillandsia landbeckii* dunes in the Atacama Desert: Evidence from radiocarbon and stable isotopes

Claudio Latorre,[1,2] Angélica L. González,[1,2] Jay Quade,[3] José M. Fariña,[1] Raquel Pinto,[4] and Pablo A. Marquet[1,2]

Received 16 August 2010; revised 23 May 2011; accepted 9 June 2011; published 14 September 2011.

[1] Extensive dune fields made up exclusively of the bromeliad *Tillandsia landbeckii* thrive in the Atacama Desert, one of the most extreme landscapes on earth. These plants survive by adapting exclusively to take in abundant advective fog and dew as moisture sources. Although some information has been gathered regarding their modern distribution and adaptations, very little is known about how these dune systems actually form and accumulate over time. We present evidence based on 20 radiocarbon dates for the establishment age and development of five different such dune systems located along a ~215 km transect in northern Chile. Using stratigraphy, geochronology and stable C and N isotopes, we (1) develop an establishment chronology of these ecosystems, (2) explain how the unique *T. landbeckii* dunes form, and (3) link changes in foliar $\delta^{15}N$ values to moisture availability in buried fossil *T. landbeckii* layers. We conclude by pointing out the potential that these systems have for reconstructing past climate change along coastal northern Chile during the late Holocene.

Citation: Latorre, C., A. L. González, J. Quade, J. M. Fariña, R. Pinto, and P. A. Marquet (2011), Establishment and formation of fog-dependent *Tillandsia landbeckii* dunes in the Atacama Desert: Evidence from radiocarbon and stable isotopes, *J. Geophys. Res.*, *116*, G03033, doi:10.1029/2010JG001521.

1. Introduction

[2] Many researchers have examined extreme environments intensively for clues as to how living organisms cope and evolve under near-abiotic conditions [*Javaux*, 2006; *Lillywhite and Navas*, 2006; *Peck et al.*, 2006]. These studies range in scale from the smallest microorganisms to macroscopic plants and animals and their modification of the landscape [*Dietrich and Perron*, 2006]. Such a major modification of otherwise barren landscapes occurs in the Atacama Desert of northern Chile where extensive areas are colonized exclusively by "tillandsiales," unique fog-dependent ecosystems that form distinct dune fields [*Rundel et al.*, 1997; *Pinto et al.*, 2006; *Westbeld et al.*, 2009; *Borthagaray et al.*, 2010].

[3] Abundant mono-specific stands of the bromeliad *Tillandsia landbeckii* are commonplace on the inner coastal landforms of the Atacama (Figure 1), an extreme hyperarid environment often used as an analog for the surface of Mars [*McKay et al.*, 2003]. These unique, functionally root-less (epiarenitic) plants survive through a series of specialized adaptations, such as Crassulacean Acid Metabolism (CAM) and interwoven aciculate leaves adorned with water-absorbing trichomes [*Rundel et al.*, 1997]. Indeed, *Rundel et al.* [1997] proposed that *T. landbeckii* propagules disperse so that an entire band or "dune" forms asexually as ramets arise from a single genet. This strategy would allow the plants to quickly colonize favorable environments as fog-water input fluctuates over time.

[4] *Tillandsia landbeckii* dunes are unique ecosystems that constitute single units with distinct natural boundaries through which energy and nutrients are exchanged readily. They are supported almost exclusively by fog with dew playing a minor role [*Westbeld et al.*, 2009]. Too little water and the plants die by dehydration but studies on bromeliads have shown that too much moisture (aside from favoring the growth of phytopathogens) can cause a surface tension film to form, collapsing the trichomes over the stomates and interfering with gas exchange essentially reducing CO_2 uptake rates [*Benzing and Renfrow*, 1971; *Benzing et al.*, 1978; *Martin*, 1994]. Water thresholds for *T. landbeckii*, however, have yet to be established empirically.

[5] Nevertheless, water availability is a key controlling aspect through fog interception by the exposed plant surface [*Borthagaray et al.*, 2010]. A recent mathematical model demonstrates how the wavelength of the typical banding pattern is a function of fog-water input, speed (wind), and

[1]Center for Advanced Studies in Ecology and Biodiversity, Departamento Ecologia and Laboratorio Internacional de Cambio Global, Pontificia Universidad Católica de Chile, Santiago, Chile.
[2]Institute of Ecology and Biodiversity, Santiago, Chile.
[3]Department of Geosciences, University of Arizona, Tucson, Arizona, USA.
[4]Iquique, Chile.

0148-0227/11/2010JG001521

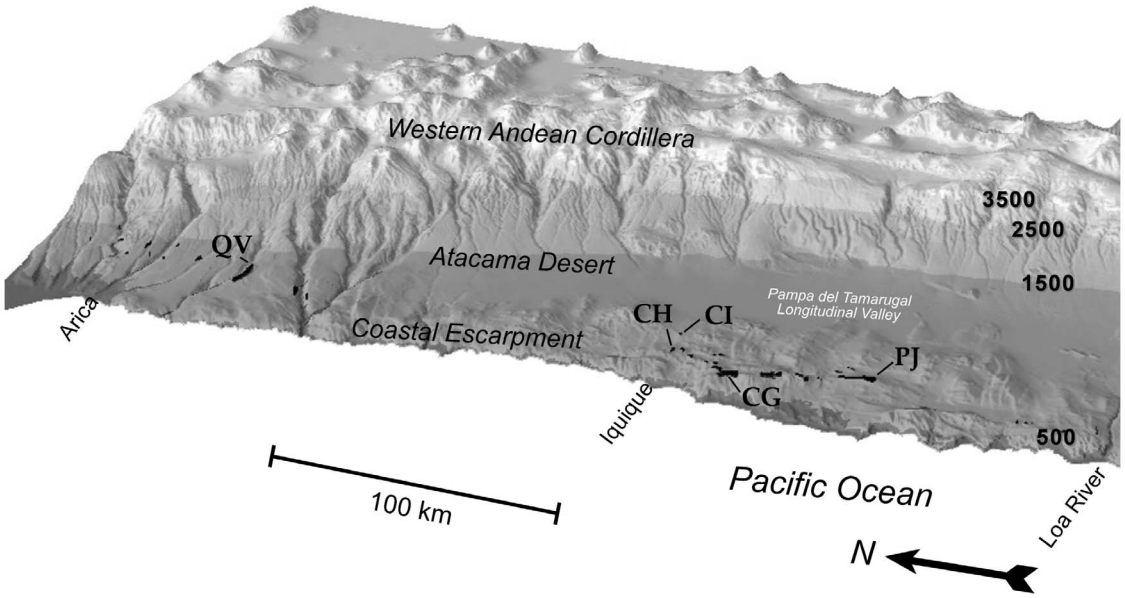

Figure 1. Oblique view of northern Chile with the distribution of known *Tillandsia landbeckii* dunefields ("tillandsiales") outlined in black [after *Pinto et al.*, 2006]. Contours are gray scaled every 1000 m (altitude in m is shown on the right). The localities discussed in the text are, from north to south, QV, Quebrada Vitor; CH, Cerro Huantajaya; CI, Cerro Isla; CG, Cerro Guanacos; PJ, Pajonales. Topographic data are from the SRTM (NASA/JPL) here shown with an exaggerated vertical scale.

topography [*Borthagaray et al.*, 2010]. Hence, the spatial distribution and formation of the 'tillandsiales' are basically constrained by the availability of fog moisture, which increases with altitude (Figure 2) starting at the marine boundary layer (which controls the height of the cloud base) until the top of the cloud deck is reached at the thermal inversion layer [*Pinto et al.*, 2006; *Garreaud et al.*, 2008; *González et al.*, 2011].

[6] The relationship between rainfall, fog and ENSO in tropical to subtropical northern Chile depends on altitude and latitude [*Garreaud et al.*, 2003; *Houston*, 2006; *Garreaud et al.*, 2008]. The central Andes receive more summer rainfall during La Niña years whereas El Niño years, which are dry on the Altiplano [*Aceituno*, 1988; *Garreaud et al.*, 2003; *Aceituno et al.*, 2009], are associated with rare winter rainfall events along the coast of northern Chile [*Houston*, 2006; *Cereceda et al.*, 2008a; *Garreaud et al.*, 2008]. The relationship between ENSO and fog intensity and frequency is less clear. A 22-year record of past fog intensity in subtropical Chile (~30°S latitude) links positive

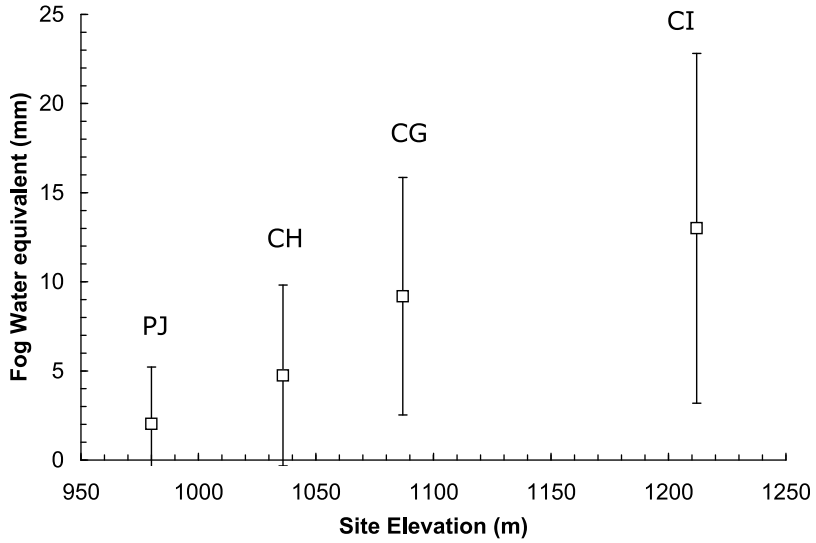

Figure 2. Fog water equivalent (in mm) plotted against altitude for the four localities discussed (see Figure 1 for abbreviations). The regression of water input on altitude is statistically significant (R^2 = 0.95, $p < 0.005$). Note that fog water input seems to level off with altitude and variance increases (see *González et al.* [2011] for data and methods).

Table 1. Geographic Location, Stratigraphy, and Radiocarbon Dates for 20 Buried *Tillandsia landbeckii* Layers Reported in This Study

	Sample	Depth From Dune Crest (cm)	Radiocarbon Lab Number[a]	^{14}C (years B.P.)	Median (cal years B.P.)[b]	+/−1 σ
		Pajonales PJ-1: S 20°43.995′- W 69°58.174′ - 983 m				
1	PJ-1-1-^{14}C	25	GX32455	1470 ± 70	1330	57/48
2	PJ-1-2-^{14}C	42	GX32399	1800 ± 80	1660	111/114
3	PJ-1-3-^{14}C	55	GX32456	1360 ± 100	1210	94/123
4	PJ-1-4-^{14}C	85	GX32400	2290 ± 40	2230	95/71
5	TILLANDSIA 1	85	GX31966	2280 ± 60	2230	97/75
		Pajonales PJ-1A: S 20°43.993′ - W 69°58.174′ - 983 m				
6	PJ-1A-5-^{14}C	78	GX32401	2150 ± 90	2080	219/203
		Pajonales PJ-2: S 20°44.031′ - W 69°58.262′ - 973 m				
7	PJ-2-4-^{14}C	80	GX32457	1470 ± 90	1330	82/140
		Pajonales P-4: S 20°42.950′ - W 69°57.895′ - 1001 m				
8	P4-1-^{14}C	130	UGAMS3048	3140 ± 25	3310	49/46
		Additional Basal Layer Dates From Pajonales				
9	TILLANDSIA 2	basal layer	GX31967	1790 ± 90	1650	124/116
10	TILLANDSIA 3	basal layer	GX31968	1680 ± 90	1520	94/115
		Quebrada Vitor QV-1: S 18°52.895′ - W 70°03.043′ - 1175 m				
11	QV-1-1-^{14}C	98	UGAMS3049	1640 ± 20	1470	50/53
		Quebrada Vitor QV-2: S 18°52.944′ - W 70°02.974′ - 1181 m				
12	QV-2-5-^{14}C	5	UGAMS3054	180 ± 20	150	126/150
13	QV-2-4-^{14}C	28	UGAMS3053	240 ± 25	200	96/46
14	QV-2-3-^{14}C	50	UGAMS3052	730 ± 20	650	17/76
15	QV-2-2-^{14}C	70	UGAMS3051	1100 ± 20	950	12/15
16	QV-2-1-^{14}C	90	UGAMS3050	1870 ± 25	1760	51/49
		Cerro Guanacos CG-1: S 20°24.064′ - W 70°04.939′ - 1100 m				
17	CG-1-1-^{14}C	125	UGAMS3055	3360 ± 25	3530	35/51
		Cerro Isla CI-1: S 20°13.477′ - W 69°54.694′ - 1222 m				
18	CI-1-1-^{14}C	80	UGAMS3056	3120 ± 25	3290	52/38
		Cerro Huantajaya CH-1: S 20°13.587′ - W 70°00.172′ - 1048 m				
19	CH-1-4-^{14}C	40	UGAMS3057	260 ± 25	280	27/125
20	CH-1-1-^{14}C	90	UGAMS3163	1980 ± 25	1870	27/44

[a]Abbreviations are GX (Geochron Labs, Boston, Massachusetts) and UGAMS (Center for Applied Isotope Studies, University of Georgia).
[b]Radiocarbon dates are calibrated using CALIB5.0.1 [*Stuiver and Reimer*, 1993], SHcal04 calibration curve [*McCormac et al.*, 2004].

(negative) phases of ENSO with high (low) fog occurrence [*Garreaud et al.*, 2008]. The key synoptic aspect controlling advective fog events appears to be the intensity and altitude of the thermal inversion that forms over the coastal Pacific as a result of the interaction between large-scale Hadley cell subsidence and the cold, northward flowing Chile-Peru (Humboldt) current. A 10-year study from northern Chile (~21°S), however, shows little or no correlation fog precipitation with ENSO, and in fact some of the foggiest years (e.g., 1997) occurred during negative phases of ENSO [*Cereceda et al.*, 2008b].

[7] Despite the clear relationship between the distribution of *T. landbeckii* dunes with fog availability, there are no studies on how these ecosystems actually form or whether the formation and persistence is related to past climate change. In this study, we use geochronology, stratigraphy and stable isotopes (C, N, O) to examine and compare active (meaning currently vegetated) versus relict (or 'dead') *T. landbeckii* dune ecosystems. Based on stratigraphic evidence, we propose a conceptual model of how these dunes are formed. We use stable carbon and nitrogen isotopes to track current and past variations in carbon sources and available moisture [*Ehleringer et al.*, 1998; *Dawson et al.*, 2002; *Ehleringer et al.*, 2002; *Swap et al.*, 2004]. Carbon isotope evidence also points to a possible explanation for the origin of distinct carbonate "cap layers" seen in many of our buried dune systems. Our results indicate that *T. landbeckii* foliar δ^{15}N in our modern systems is linked to δ^{15}N values on total N present in fog. Furthermore, we point out that fog δ^{15}N, total N concentration in fog and fog water input all appear to be related. We conclude by exploring the paleoclimatic potential of these dune systems as unique archives for past fluctuations of coastal advective fog intensity during the late Holocene.

2. Methods

2.1. Site Description

[8] We surveyed and excavated fourteen different *T. landbeckii* dunes from five of the largest and/or most isolated fields known from northern Chile (Figure 1). From north to south, these are: Quebrada Vitor (QV), Cerro

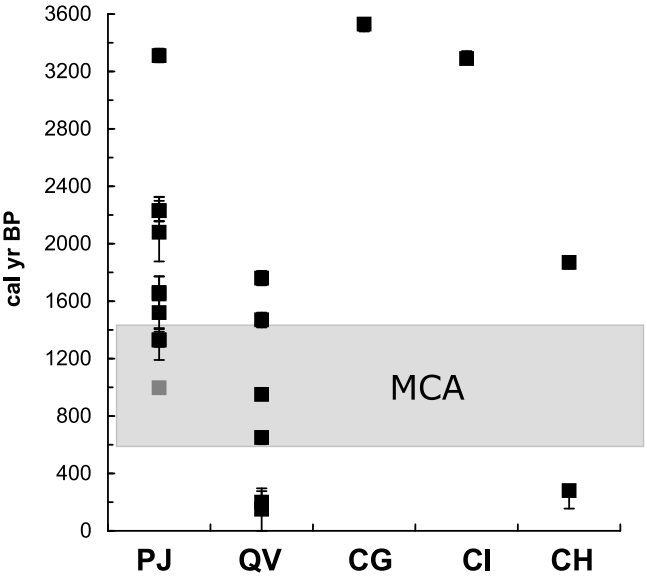

Figure 3. Time series plots and basal dates for the *T. landbeckii* dunes analyzed and dated in this study. Site abbreviations are QV, Quebrada Vitor; CH, Cerro Huantajaya; CI, Cerro Isla; CG, Cerro Guanacos; PJ, Pajonales. The gray square for the PJ series is the extrapolated age of the dune crest using the age/depth relationship plotted in Figure 4 and represents the last time living plants occurred at this site. Also indicated is the extent of the MCA or Medieval Climate Anomaly (shaded), a period of sustained "la Niña-like" conditions [also see *Graham et al.*, 2007].

Huantajaya (CH), Cerro Isla (CI), Cerro Guanacos (CG) and Pajonales (PJ) (Table 1). Site position within the cloud deck is critical and therefore altitude is a key factor that explains how much moisture is received at a given locality (Figure 2), We also sampled *T. landbeckii* dune systems (at PJ and QV) that are "dead" or relict ecosystems. These dunes persist on the landscape but without living plants on the surface, the whole of the dune still held in place by dead vegetation.

[9] The geography of coastal northern Chile can be divided into a narrow coastal shelf (where most of the major cities, such as Iquique, are located), a steep 800–1000 m coastal escarpment, and a N-S oriented longitudinal basin (Figure 1). Lower to middle Miocene alluvial gravels outcrop at QV whereas lower to middle Jurassic marine limestones to upper Jurassic conglomerates and littoral facies occur in the Iquique area. In places, these are intruded by late Jurassic to Cretaceous batholiths [*SERNAGEOMIN*, 2003]. The entire region is tectonically very active [*Gonzalez et al.*, 2006].

[10] Regional climate is hyperarid and direct rainfall is practically non-existent. Although infrequent, brief but intense rainfall events can occur during El Niño years [*Houston*, 2006]. Fog is much more frequent year-round but it is most intense during the winter months from June to August [*Cereceda et al.*, 2008b]. Moisture from fog is essential in maintaining the isolated, diverse and highly endemic plant communities know locally as "*Lomas*" found between 400 and 900 m throughout coastal northern Chile and southern Peru [*Rundel et al.*, 1991; *Marquet et al.*, 1998]. *T. landbeckii* dunes, when present, typically occur between 950 and 1300 m and are located well above any *Lomas* vegetation.

2.2. Analytical Methods

[11] For each excavated dune, strike and dip measurements were taken on the saltational (stoss) surfaces and geographic position and elevation noted using a barometric GPS. Dunes were excavated down to bedrock or to the underlying efflorescent salt crust (usually >1.5 m). Stratigraphy was described for each excavated section and the resulting exposed organic horizons were carefully collected in the field and sealed in plastic bags. Overlying carbonate layers were sampled using a trowel, focusing on the purest (most sand-free) layers. We also sampled living *T. landbeckii* plants from each locality with the exception of those at PJ-1, PJ-2 and QV, which are dead stands.

[12] We ^{14}C-dated a total of 20 buried *T. landbeckii* layers to develop a chronology of past dune establishment and buildup (Table 1). These buried layers are extraordinarily well preserved and many have easily recognizable leaves and stems. Emphasis was placed on the largest dunes for radiocarbon dating, as these were potentially the oldest as well because successive stages of growth, dieback and colonization could explain the unusual stratigraphy and increased height with age (see Figure 5 and section 4.1). A sample of *T. landbeckii* leaves from every basal layer from nine of these dunes was dated. Conventional radiocarbon dating on 1–3 g of leaf tissue was performed at Geochron Labs (the "GX series") with further accelerator mass spectrometry (AMS) dating done at the Center for Applied Isotopes of the University of Georgia (the "UGAMS series"). All radiocarbon dates were converted to calendar years before 1950 (cal years B.P.) using CALIB5.0.2 [*Stuiver and Reimer*, 1993; *Stuiver et al.*, 1998] with the SHCal04 calibration curve [*McCormac et al.*, 2004].

[13] We determined δ^{15}N (AIR) values for fog water, previously collected for a different study [see *González et al.*, 2011], on total N content. Three samples of fog water per site (PJ, CG, CI and CH) were collected at different times of the year. Fog water δ^{15}N values were measured on 500 μL of dried water into tins, 50 μL at a time, on a ThermoFinnigan Delta V Advantage Isotope Ratio Mass Spectrometer (IRMS) coupled to a Carlo Erba NC2500 Elemental Analyzer (EA) via continuous flow at the Cornell Stable Isotope Laboratory (COIL), Ithaca NY.

[14] Buried plant δ^{13}C (VPDB) values were measured directly on *T. landbeckii* tissue in preparation for radiocarbon dating and fractionation correction. Additional δ^{13}C and δ^{15}N analyses were performed on whole tissue for buried plants (which were often very degraded) and on living plant leaf/stem tissue using a Finnigan Delta Plus continuous-flow Isotope Ratio Mass Spectrometer (IRMS) and elemental analyzer (Thermo Electron, Waltham, MA) at the Stable Isotope Laboratory, University of Arkansas. Isotope ratios were calculated and normalized by using a number of in-house and international standards (i.e., bovine liver).

[15] Carbonate samples (from buried *T. landbeckii* dunes) were heated at 250°C for three hours in vacuo and analyzed with an automated sample preparation device (Kiel III) attached directly to a Finnigan MAT 252 mass spectrometer at the University of Arizona. Precision of repeated standards

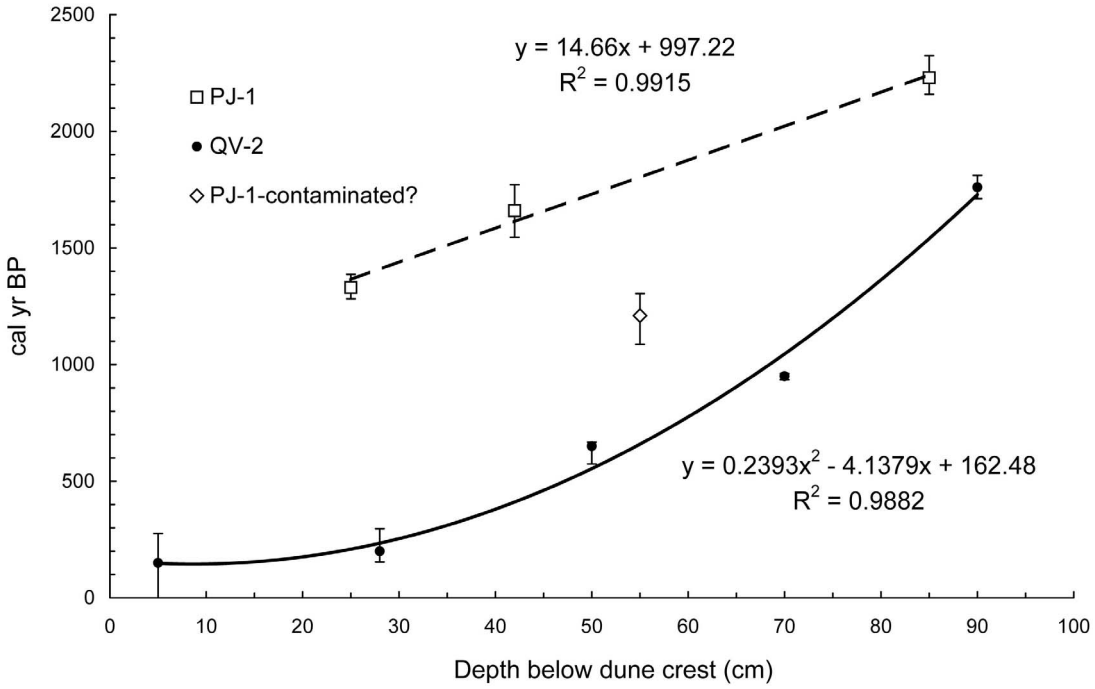

Figure 4. Age-depth curves for two relict (i.e., no living plants at these sites today) *T. landbeckii* dune systems located at Pajonales (section PJ-1) and Quebrada Vitor (QV-2). See Figure 1 for site locations. The full stratigraphy for these curves and other sites is available in the auxiliary material Figures S1–S8.

is ±0.11‰ for δ^{18}O (VPBD) and ±0.07‰ for δ^{13}C (VPDB) (at 1σ). One-way and two-way ANOVA were used to assess the statistical differences in δ^{13}C and δ^{15}N between modern sites and between modern versus buried *T. landbeckii* layers.

3. Results

3.1. Stratigraphy and Chronology

[16] All *T. landbeckii* dune crests strike irregularly N to N-NW typically perpendicular to the predominant westerly winds. Usually buried within the dune are several *T. landbeckii* layers that dip 4–8° to the W-SW. Parallel to these layers are several discrete (1–2 cm thick) layers of calcium carbonate, often capping buried *T. landbeckii* layers although many of the carbonate layers observed also occurred without any visible plant remains. The number of buried *T. landbeckii* layers observed in our sections also tended to increase with dune height (to a maximum of ~1.6 m). Dune matrix is mostly fine to medium-fine litharenites with bedding that tends to either parallel the *T. landbeckii* layers or is typically horizontal. Cross bedding was visible only in the basal portions of a few of our sections where few or no plant remains occurred (see Figures S1–S8 in the auxiliary material).[1]

[17] Twenty ^{14}C dates from five localities indicate that *T. landbeckii* dune establishment occurred at CG, CI, and at PJ over 3200 years ago. Ages on buried *T. landbeckii* basal layers for some of the largest dunes (~1.6 m high) at these sites are 3510, 3290 and 3310 cal years B.P., respectively (Table 1 and Figure 3). The relict (dead stands) *T. landbeckii* dunes at PJ and QV are younger. Three basal dates from the largest dunes do not exceed 2230 cal years B.P., whereas other dunes (PJ-2) display considerably younger basal dates (1330 cal years B.P.). Two basal dates from QV also indicate younger ages of 1760 (QV-2) and 1470 cal years B.P. (QV-1). The older QV-2 date is coeval (at 2 standard deviations) with a basal date of 1870 cal years B.P. from CH and with two other basal dates at PJ (Table 1).

[18] Nine radiocarbon dates provide the age-depth relation for two of the "dead" *T. landbeckii* dunes (see Figures S1 and S2). Excluding one sample (PJ-1-3-^{14}C, Table 1), the three dates from section PJ-1 indicate that age increases linearly with depth from the dune crest at the rate of ~15 cm/yr (Figure 4). The excluded date from this sequence exhibits a significant age reversal (e.g., it is too young) in comparison to the linear relationship that exists between the other three dates, and may be due to sample mixing from the younger layers. Linear extrapolation of the best fit for the three dates at PJ-1 gives an age of ~1000 cal years B.P. for the crest of the dune (plotted as a gray square in Figure 3).

[19] Five dates from a relict or "dead" *T. landbeckii* dune at QV-2 show slow accumulation rates over 20 cm/yr near the base of the section that increase to 1–2 cm/yr at the top. *T. landbeckii* dunes at QV have slightly younger basal dates than those at Pajonales (Figures 3 and 4). Whereas the largest dunes at Pajonales probably became relict by ~1000 cal years B.P., those at QV remained active until the 19th century (150 cal years B.P.).

[1] Auxiliary materials are available in the HTML. doi:10.1029/2010JG001521.

Table 2. Stable Isotope Analyses for 24 Samples of Living and Seven Samples of Buried *T. landbeckii* Plants and Average Fog Water $\delta^{15}N$

Locality[a]	Sample Type	$\delta^{13}C$	$\delta^{15}N$	Average $\delta^{13}C$ (±sd)	Average $\delta^{15}N$ (±sd)
CG-1	leaf	−13.81	−4.00		
CG-2	leaf	−13.33	−3.47	leaf	leaf
CG-3	leaf	−13.77	−4.55	−13.64 ± 0.27	−4.01 ± 0.54
CG-1a	stem	−14.27	−1.38		
CG-2a	stem	−13.34	−2.21	stem	stem
CG-3a	stem	−13.73	−1.44	−13.78 ± 0.47	−1.68 ± 0.46
CH-1	leaf	−12.49	−3.67		
CH-2	leaf	−13.38	−2.35	leaf	leaf
CH-3	leaf	−14.01	−1.78	−13.29 ± 0.76	−2.60 ± 0.97
CH-1a	stem	−13.17	−2.09		
CH-1b	stem	−13.39	−0.28	stem	stem
CH-1c	stem	−12.76	−0.89	−13.11 ± 0.32	−1.09 ± 0.92
CI-1	leaf	−12.82	−1.06		
CI-2	leaf	−13.77	−2.72	leaf	leaf
CI-3	leaf	−13.44	−2.76	−13.34 ± 0.48	−2.18 ± 0.97
CI-1a	stem	−14.05	−0.93		
CI-2a	stem	−13.68	−1.52	stem	stem
CI-3a	stem	−14.07	−0.78	−13.93 ± 0.22	−1.08 ± 0.39
PJ-1	leaf	−13.42	−0.39		
PJ-2	leaf	−13.77	0.40	leaf	leaf
PJ-3	leaf	−13.25	0.94	−13.48 ± 0.27	0.32 ± 0.67
PJ-1a	stem	−13.90	1.22		
PJ-2a	stem	−13.84	1.78	stem	stem
PJ-3a	stem	−13.92	2.56	−13.89 ± 0.04	1.85 ± 0.67
PJ-1a	buried leaves	−10.69	−1.41		
PJ-1a	buried leaves	−10.54	−4.88		
PJ-1a	buried leaves	−11.06	−3.91	leaf	leaf
PJ-1a	buried leaves	−10.49	−6.36	−10.73 ± 0.27	−3.83 ± 1.53
PJ-2	buried leaves	−11.10	−3.56		
PJ-2	buried leaves	−10.81	−3.69		
PJ-2	buried leaves	−10.45	−3.00		
			Fog Water $\delta^{15}N$ (n = 3 per Site)		
CG	total N fraction in water				N fraction was too small for a reliable measurement
CH	total N fraction in water				−1.02 ± 2.06
CI	total N fraction in water				0.31 ± 0.15
PJ	total N fraction in water				2.58 ± 1.11

3.2. The $\delta^{13}C$ and $\delta^{18}O$ Values of Living Versus Buried *T. landbeckii* Layers and Associated Carbonates

[20] The $\delta^{13}C$ values from living *T. landbeckii* plants (n = 24 samples) range from −12.5 to −14.3‰ with an average of −13.6 ± 0.4‰ (Table 2). At most sites, excepting CH, stems were apparently slightly more negative (<0.5‰) values than their counterpart leaves. None of these differences, however, are significant either between localities (two way ANOVA: $F_{16,0.95} = 2.08$; $p = 0.143$) or across tissue types (two-way ANOVA: $F_{16,0.95} = 2.05$; $p = 0.171$). There was also no significant interaction between factors (tissue type, locality) (two-way ANOVA, $F_{16,0.95} = 1.03$, $p = 0.406$).

[21] In contrast, the $\delta^{13}C$ values of buried *T. landbeckii* leaves range from −14.8 to −10.4‰ (n = 16) with a mean of −11.6 ± 1.3‰ (Table 2). These values are slightly higher (by 2‰ on average) and exhibit higher variance when compared to the modern *T. landbecki* stands sampled from the same localities. A one-way ANOVA between modern and buried samples indicates that this difference is statistically significant $F_{14,0.95} = 21$, $p < 0.0001$).

[22] We also sampled the corresponding loosely carbonate-cemented sand layer that typically caps each one of the buried *T. landbeckii* layers. Although carbonate content is low (10–20%), these caps display $\delta^{13}C$ values with an even

Table 3. Paired $\delta^{13}C$ and $\delta^{18}O$ Values on Buried Carbonate Layers and Corresponding Plant Layer

Sample[a]	Depth From Dune Crest[b] (cm)	$\delta^{13}C_{PDB\ (plant)}$	$\delta^{13}C_{PDB\ (CaCO3)}$	$\delta^{18}O_{PDB\ (CaCO3)}$
PJ-1-1	20, 25	−12.9	0.81	1.07
PJ-1-2	40, 42	−13.2	0.40	−3.50
PJ-1-3	50, 55	−13.5	0.63	2.46
PJ-1-4	82, 85	−14.8	1.18	1.80
PJ-1A-1	25, 28	−10.69	0.55	1.47
PJ-1A-3	50, 55	−11.06	0.58	1.35
PJ-1A-4	65, 68	−10.49	0.94	0.79
PJ-1A-5	75, 78	−12.3	0.53	1.46
PJ-2-1	10, 12	−11.10	−0.21	0.86

[a]See Table 1 for site abbreviations.
[b]Numbers correspond to depth of carbonate and depth of paired buried plant layer.

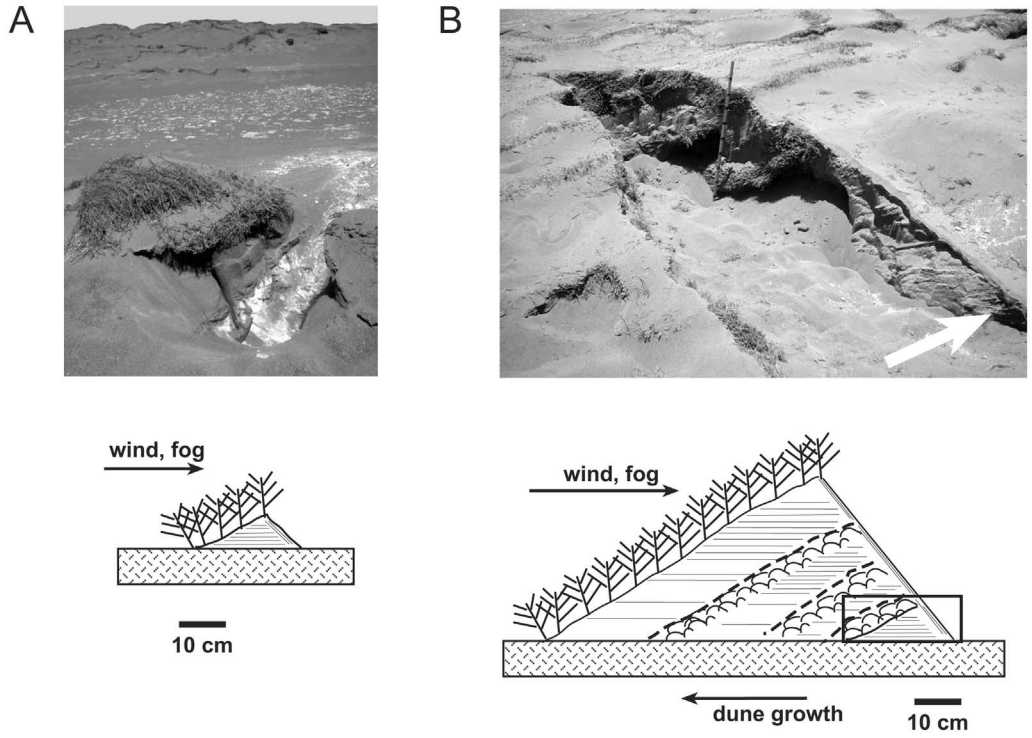

Figure 5. A plausible explanation for how *T. landbeckii* dunes form based on stratigraphy and geochronology. (a) (top) Photograph of an incipient *T. landbeckii* dune at Pajonales as it forms on the efflorescent anhydrite crust (white layer underneath dune and in the middle foreground, which is sand free). The interwoven plants grow on the slope facing the wind and trap sand downwind in horizontal layers therefore maximizing exposure to oncoming fog (rock hammer for scale). (bottom) Schematic representation of the same dune indicating wind and moisture direction (black arrow) and prominent bedding of sand layers as well as the salt crust underneath the dune (hatched pattern). (b) (top) Photograph of a trench dug into the slip-face of a mature, large (~1 m) *T. landbeckii* dune at Pajonales (section PJ-2). At least four buried organic layers are apparent (vertical rod is marked every 10 cm) all of which dip ~10° to the west. White arrow points to a buried incipient organic layer of *T. landbeckii* that likely originated the dune, dated to 1470 ± 90 ^{14}C years B.P. (see Table 1). Also visible is the corresponding cap carbonate. (bottom) Schematic representation of a mature dune. The initial stage, box outline, is now completely buried underneath horizontally to slightly westward dipping sand layers and has developed a prominent cap carbonate (dashed line). Several more layers have now developed as the dune increases in height and grows into the wind.

narrower range of −0.2 to +0.9‰ (n = 11), with a mean of +0.6‰ (Table 3). The δ^{18}O values for these cap carbonates range from +0.6 to +2.2‰ (Table 3).

3.3. The δ^{15}N Values From Fog Water

[23] δ^{15}N analyses on total N fraction in fog water revealed average values that span from −1.0 ± 2.1 (at CH) to +2.6 ± 1.1‰ (at PJ). The highest values occur at the lowest elevation site (PJ) whereas sites at higher elevations display on average, more negative values (Table 2). There was not enough N content in the fog water collected at CG to obtain reliable δ^{15}N values.

3.4. Living Versus Buried *T. landbeckii* δ^{15}N Values

[24] The δ^{15}N values from living plants exhibit a considerable degree of variation, with those at PJ returning the highest values (+2.6‰) and those from CG the lowest (−4.6‰) (Table 2). This range of values (>7‰) is considerably larger than that previously reported for *T. landbeckii* [*Evans and Ehleringer*, 1994; *Ehleringer et al.*, 1998]. There is significant variation between tissue types where stems evince δ^{15}N values that are significantly more enriched in ^{15}N (on the order of 1–2 ‰) than the respective leaf δ^{15}N values (two-way ANOVA, $F_{16,\ 0.95} = 29.41$, $p < 0.0001$). There are also significant differences across sites ($F_{16,\ 0.95} = 31.59$, $p < 0.0001$). As with the δ^{13}C values, there is no significant interaction across factors (locality, tissue type) ($p = 0.55$).

[25] Buried *T. landbeckii* leaves from the relict dunes at PJ have δ^{15}N values as low as −6.4 ‰ (Figure 7 and Table 2). This contrasts with the living plants found there that exhibit δ^{15}N values on average of +1.1 ‰, almost 5‰ more than their buried counterparts which average −3.8 ‰. These differences are statistically significant (Tukey's Multiple Comparison Test, $q = 5.972$, $P < 0.05$). Indeed, the average values of these

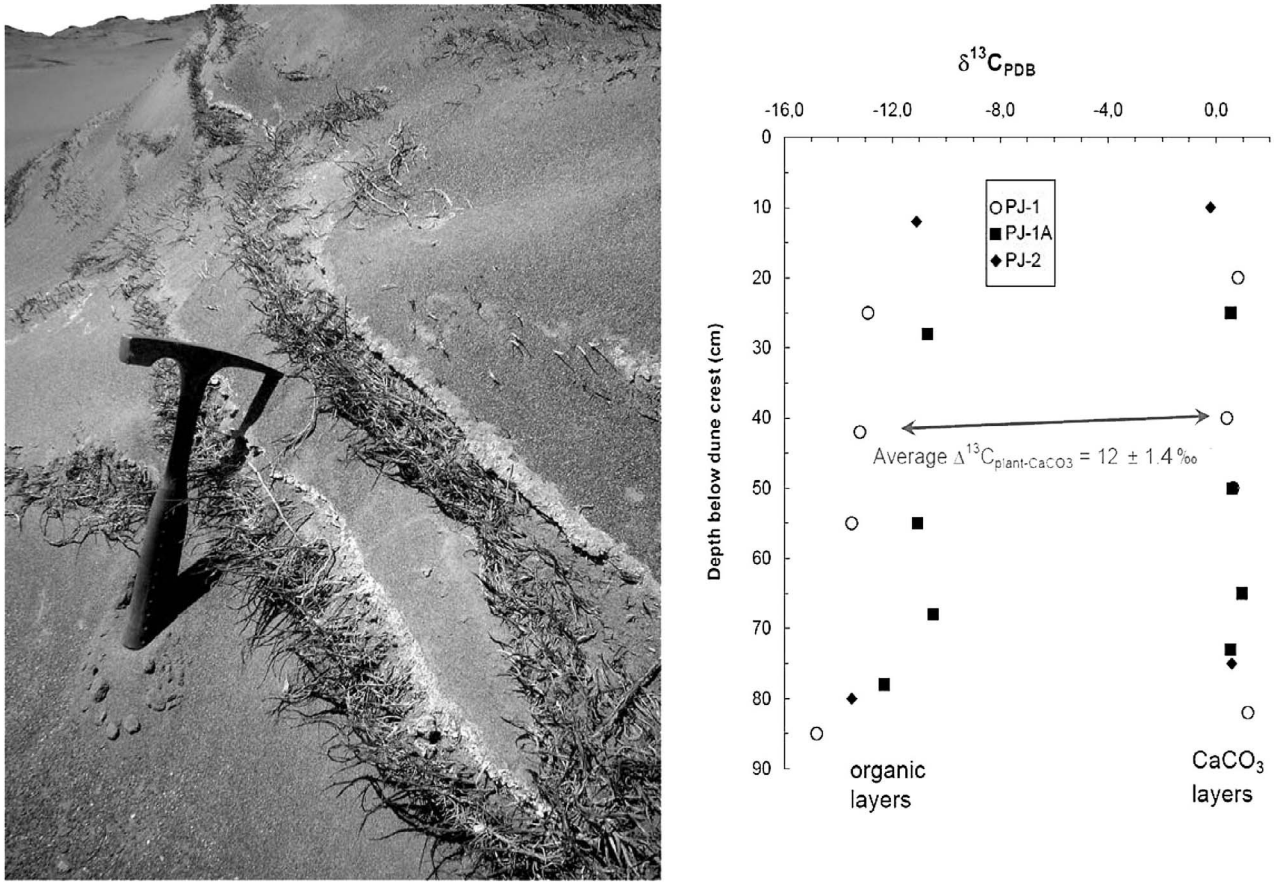

Figure 6. (left) Photograph of a vertical profile along the slipface of a relict *Tillandsia landbeckii* dune located at Pajonales (section PJ-1A). At least two westward dipping, distinct buried layers of *T. landbeckii* are visible. Also visible are the 2–3 cm thick layers of calcium carbonate that build up on top of each *T. landbeckii* layer. Rock hammer is ~30 cm in length. (right) A $\delta^{13}C$ versus depth plot indicating the isotopic spread of buried *T. landbeckii* horizons and their respective carbonate "caps" (data from sections PJ-1, PJ-1A and PJ-2, also see Table 1).

buried leaves are similar to living plants collected at CG, CH and CI.

4. Discussion

4.1. How *T. landbeckii* Dunes Grow and Cap Carbonate Formation

[26] Our radiocarbon chronology indicates that the largest *T. landbeckii* dune fields established over 3200 years ago (Figure 3). For those profiles in which we dated all layers preserved within the dune, sediment accumulation rates varied from relatively constant (at PJ-1) to variable over time (section QV-2) (Figure 4). *T. landbeckii* dune bedding planes and internal stratigraphy are highly atypical for windblown dunes, which typically are internally cross-bedded. This unusual stratigraphy results from the way these landforms are generated. *T. landbeckii* plants act as sand traps, in a landscape where there is little sand except where these plants grow. As sand accumulates downwind from these plants in near-horizontal layers, they spread over the sand, thereby maximizing their profile toward the wind and fog, and creating a small incipient dune-like structure (Figure 5, see also *Borthagaray et al.* [2010]). Eventually, the plants die and/or are buried and windblown sand accumulates parallel to the now dead mat. As the dead plants are buried by sand, calcium carbonate accumulates within the sandy matrix over the plants as a distinct cap. Thereafter, a new *T. landbeckii* mat grows over the wind-facing slope of the dune, generating a new layer of plants. Successive stages of growth, dieback and colonization explain the unusual stratigraphy (and increased height with age) seen in these dunes (Figure 4).

[27] The close stratigraphic relationship between the carbonates and the buried *T. landbeckii* layers in our PJ sections (Figure 6) implies that the carbonates are organically derived (i.e., CO_2-respired) rather than forming from detrital carbonate reworked from distant sources. An organic origin for the carbonates is also strongly supported by the $\delta^{13}C$ values, which in soils display a predictable difference ($\Delta\delta^{13}C$) from the average $\delta^{13}C$ of local plant cover. Modeling of the soil system [*Cerling*, 1984; *Quade et al.*, 2007] shows that plants strongly influence the isotopic composition of soil carbonate and that the two will differ by 13–15‰ in most soils depending on local soil conditions such as temperature, soil depth, and soil respiration rates. The observed $\Delta\delta^{13}C = -12 \pm 1.4$ ‰ for nine organic matter/

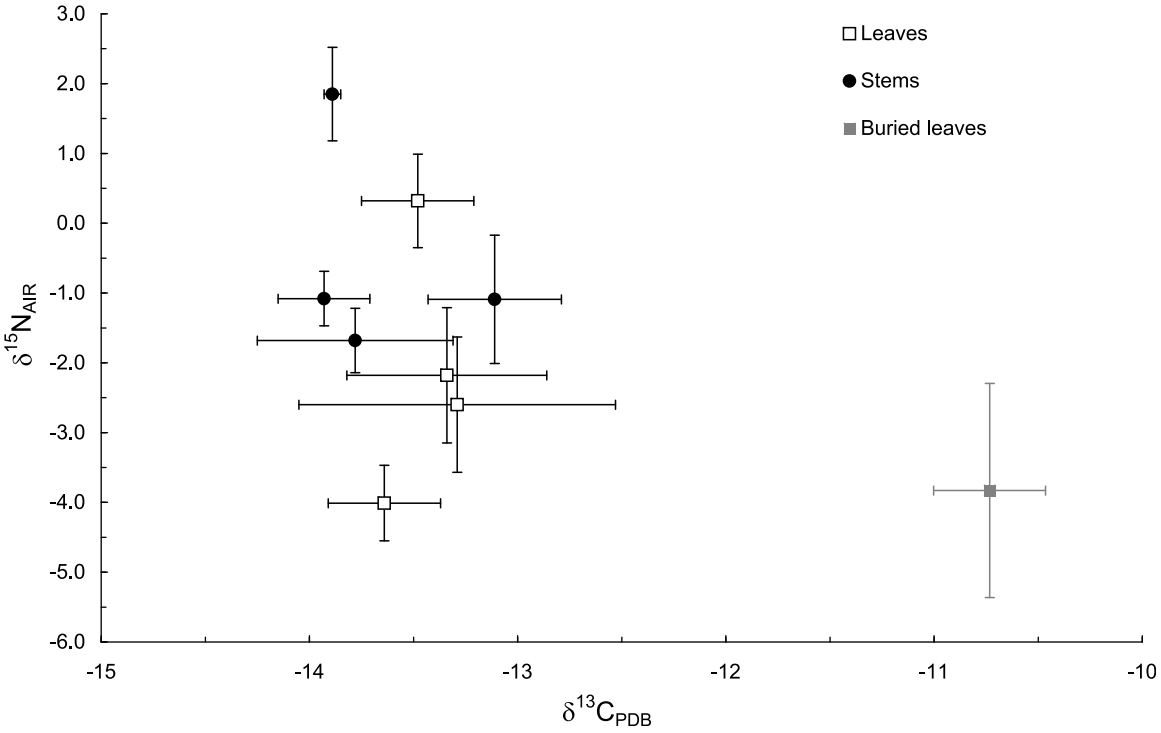

Figure 7. A plot of δ^{13}C versus δ^{15}N values obtained on living (all sites) and buried *T. landbeckii* (all from PJ) leaves and stems. The buried samples from Pajonales are much more depleted in ^{15}N and δ^{13}C values are offset by ~3‰ from their modern counterparts. See also Tables 1 and 2 for stable isotope data.

carbonate pairs closely matches the expected values for soils. Using the soil diffusion model described by *Cerling* [1984] and *Quade et al.* [2007] for our specific site conditions (altitude = 1000 m; mean annual temperature = 18°C; moderate soil respiration rates of 6 mmoles/m^2/hr), we obtained estimates of δ^{13}C values for soil carbonates of −0.5 to +1.9‰, encompassing our observed range of −0.2 to +0.9‰. According to this model, the mean δ^{13}C value for soil organic matter of −12.2‰ should produce δ^{13}C values for carbonates of +0.8‰, very close to the average carbonate δ^{13}C value we observed (0.6‰). δ^{13}C values of soil carbonate formed in equilibrium with the atmosphere should be >+2.0‰. Hence, we view the development of carbonate and presence of plants as clearly associated processes. How this occurs exactly may have to do with oxidation of calcium oxalate (weddelite) commonly present in cacti and other CAM succulents in general [*Rivera and Smith*, 1979; *Franceschi and Nakata*, 2005; *Garvie*, 2006]. The presence of calcium oxalate raphide crystals are common features of the vegetative and reproductive organs of the Bromeliaceae and the Tillandsoideae [*Proenca and Das Gracas Sajo*, 2008]. Bio-oxidation and later atmospheric conversion of weddelite to calcite in fallen, decaying giant saguaro cacti (*Carnegia gigantea*) form distinct white carbonate crusts in the Sonoran desert [*Garvie*, 2003]. Perhaps a similar process may also be responsible for the formation of the cap carbonates seen in our stratigraphic sections but will require further study of calcium oxalate biomineralization processes in *T. landbeckii*.

[28] In general, living *T. landbeckii* δ^{13}C values are much more conserved (e.g., lower variance) than the buried plants (Table 2). The δ^{13}C varies with depth between values as low as −14.8‰ and as high as −10.5‰ (Table 3). On average, however, buried layers are shifted by 2‰ toward more positive values than the living samples. The reason is most likely the addition of fossil carbon to the atmosphere during the twentieth century which has shifted the average $\delta^{13}C_{atm}$ from −7 to −9‰ (the "Suess" effect [see *Keeling*, 1979]). This 2‰ difference is readily apparent in Figure 7.

[29] The δ^{18}O (VPDB) values of the cap carbonates (+0.6 to +2.2‰) are quite high compared to most soil carbonate values globally, which typically are less than 0‰. The high δ^{18}O (VPDB) values of these carbonates are consistent, however, with the hyperarid coastal setting of the study site and similar to values observed in near-coastal soil carbonates found further south in the Atacama [*Quade et al.*, 2007].

4.2. Natural Abundance of δ^{15}N in *T. landbeckii*

[30] Foliar δ^{15}N values from Lomas fog oases of the Atacama desert have been shown to be highly enriched in ^{15}N and unrelated to marine and/or atmospheric sources of nitrogen [*Evans and Ehleringer*, 1994]. As mentioned by *Evans and Ehleringer* [1994], however, *T. landbeckii* does not possess an effective root system for soil mineral N uptake and obtains all nitrogen from atmospheric sources. Thus, the large spread in δ^{15}N values observed in our living plants is surprising (Figure 7), and must reflect variations in atmospheric nitrogen input.

[31] The natural abundance of δ^{15}N in plants is due to the net effect of a range of processes both biological and geochemical [*Dawson et al.*, 2002]. Several large data sets

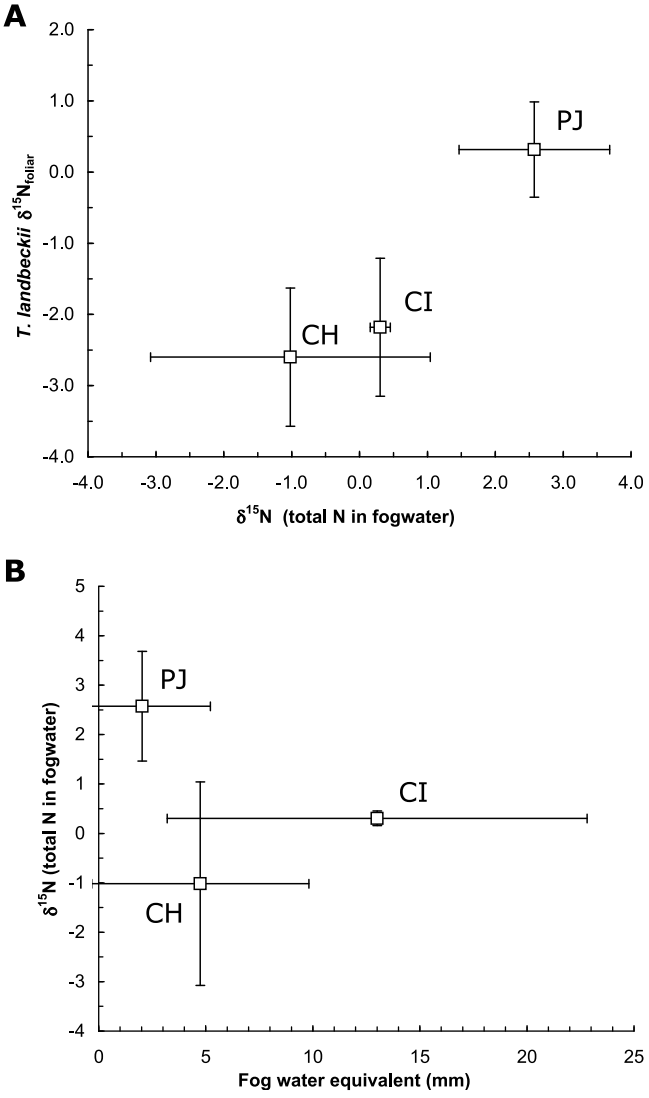

Figure 8. (a) A plot of living *T. landbeckii* foliar δ^{15}N versus δ^{15}N on total N contained in fog water. (b) Fog water equivalent (in mm) versus δ^{15}N on total N in fog water for three of our sites (abbreviations are CG, Cerro Guanacos; CH, Cerro Huantajaya; CI, Cerro Isla;, PJ, Pajonales). PJ is the locality that receives the least amount of fog and has very high δ^{15}N values. The differences between the other two sites are not significant. Note the large amount of variance in fog water amount and very small δ^{15}N error bars on the average values at CI- the highest locality. All averages are based on three measurements each.

indicate that foliar δ^{15}N values vary inversely with moisture availability and rainfall [*Handley et al.*, 1999; *Swap et al.*, 2004]. A recent study from southern Africa also correlated increasing δ^{15}N to decreased rainfall across a large latitudinal gradient [*Wang et al.*, 2010]. As previously stated, fog measurements using passive water collectors at CI, CG, CH and PJ indicate that annual mean effective moisture is highest (but also most variable) at CI, followed by CG, and CH with PJ showing the least amount of fog (Figure 2). Living *T. landbeckii* δ^{15}N values from CI, CG and CH are also significantly lower (average δ^{15}N = −2.1 ‰) than those from the PJ site (average δ^{15}N = +1.1 ‰) (Figure 7).

[32] Practically no studies exist that have examined the relationship between δ^{15}N and total N content in fog water. Although the number of samples analyzed is preliminary, our study implies a relationship between *T. landbeckii* foliar δ^{15}N and δ^{15}N on total N content in fog water (Figure 8a). In turn, fog water δ^{15}N values are highest at Pajonales which also receives the lowest amount of fog water (Figure 8b). Large errors associated with highly variable (but frequent) fog events at Cerro Isla coupled with the fact that we were not able to retrieve enough water in the N depleted fog of Cerro Guanacos for analyses, preclude us from concluding if there is a trend between fog intensity/frequency at a given site and the lower fog δ^{15}N values. This will require further research into the mechanisms and considerably more data.

[33] Yet, given the very negative δ^{15}N values observed for the relict *T. landbeckii* dune systems present at PJ (average of −3.8 ‰), it is plausible that these currently relict systems grew under considerably wetter conditions than their living, much more spatially restricted counterparts. The δ^{15}N values of the buried layers at PJ are in fact comparable to those seen at CG and CI today, which receive between 4.5 to 6 times more fog than the modern samples found at Pajonales. We are cautious, however, of these results until more stable isotope analyses on present-day fog N content are performed and the mechanisms of variation better understood.

4.3. A New Paleoclimate Record for Past Variations in Advective Fog?

[34] Radiocarbon dates from the largest *T. landbeckii* dunes at CG, PJ and CI indicate that these ecosystems were established by 3200 cal years B.P. (Figure 3). This chronology also demonstrates that the largest of the "dead" *T. landbeckii* dunes formed 2230 years ago and were periodically active until ~1000 years ago. These ages are coeval with a period of heightened climatic variability observed during the late Holocene and associated with large amplitude ENSO events at high frequencies [*Moy et al.*, 2002]. After this period, El Niño-driven lithic concentrations in a core taken offshore central Peru indicate that ENSO variability dwindled practically to zero between 1200 and 800 cal years B.P. [*Rein et al.*, 2004]. This later period, part of the Medieval Climate Anomaly (MCA) was characterized by semi-permanent La Niña conditions [*Graham et al.*, 2007]. During modern la Niña events, upwelling increases along the Chilean coastline due to an increased southerly winds [*Garreaud et al.*, 2008; *Garreaud and Falvey*, 2009]. In turn, this would lower the altitude of the marine boundary layer, effectively reducing the height of the fog bank. Although too much moisture could have caused the demise of the extensive *T. landbeckii* dune fields at Pajonales, the foliar δ^{15}N values of the buried layers are within the range of living *T. landbeckii* plants found today at slightly higher elevations (e.g., Cerro Guanacos and Cerro Isla).

[35] The extensive Pajonales system may have developed at a time when fog events were much more frequent than today, implying that the fog bank was at a lower elevation than it occurs at present. Alternatively, a major change in marine N sources during the late Holocene could explain the lower foliar δ^{15}N values observed in the buried layers at

Pajonales. Such changes, however, have not been documented on these timescales in sediment records off north-central Chile [*De Pol-Holz et al.*, 2007].

5. Conclusions

[36] In this study, we use stratigraphic and geochronological evidence to propose an explanation of how *T. landbeckii* dunes form. Contrary to wind-blown dunes, the systems studied here actually grow against the main wind direction, which would explain their unusual layered stratigraphy. We also examined a number of parameters preserved in the buried *T. landbeckii* layers, including stable carbon and nitrogen isotopes. Stratigraphic and stable carbon isotope evidence clearly points to a link between *T. landbeckii* leaf burial and the generation of distinct "cap" carbonates. This process occurs in a similar fashion to the development of soil carbonate but instead of precipitation of biologically respired CO_2, we suspect that oxidation of calcium oxalate (weddelite) may be involved in the origin of these carbonates.

[37] The spread of $\delta^{15}N$ values observed in our study is considerably larger than those previously reported for *T. landbeckii*. Significant changes in $\delta^{15}N$ are often linked with moisture availability. In fact, we show that a positive relationship does exist between foliar $\delta^{15}N$ values and $\delta^{15}N$ values on N in fog water. In turn, our preliminary data hints at a relationship between $\delta^{15}N$ values on N in fog and fog water amount although more research is needed regarding the sources of variation of $\delta^{15}N$ values in fog. Thus, we suggest that the low $\delta^{15}N$ values seen in the buried plants of presently relict dune ecosystems in comparison to their modern counterparts (which average almost 5‰ higher) could be due to increased fog. In turn, this implies a lowered fog bank such that these plants received moisture on par with living ecosystems that are 100–150 m higher in elevation. Finally, by complementing radiocarbon dating with variations in plant $\delta^{15}N$, we point out the potential of generating a unique record of past changes in advective fog in northern Chile that could potentially span the last 3,500 years.

[38] **Acknowledgments.** We thank A. Cherkinsky, Geochron Labs and the Center for Applied Isotopes Studies (University of Georgia) for radiocarbon dates. C.L., J.M.F. and P.A.M. acknowledge funding from FONDAP 1501–0001 to CASEB (Program 4). C.L. and P.A.M. also acknowledge additional support from grants P05–002 ICM and PFB-23 to the IEB and support from CSIC -PUC grant to the LINCGlobal Program. A.L.G. was funded by FONDECYT 3090029. Additional radiocarbon dating and analyses were provided by FONDECYT 1100916 (to C.L.).

References

Aceituno, P. (1988), On the functioning of the southern oscillation in the South American sector. Part I: Surface climate, *Mon. Weather Rev.*, *116*, 505–524, doi:10.1175/1520-0493(1988)116<0505:OTFOTS>2.0.CO;2.

Aceituno, P., M. D. Prieto, M. E. Solari, A. Martinez, G. Poveda, and M. Falvey (2009), The 1877–1878 El Niño episode: Associated impacts in South America, *Clim. Change*, *92*, 389–416, doi:10.1007/s10584-008-9470-5.

Benzing, D. H., and A. Renfrow (1971), Significance of the patterns of CO_2 exchange to the ecology and phylogeny of the Tillandsioideae (Bromeliaceae), *Bull. Torrey Bot. Club*, *98*, 322–327, doi:10.2307/2483971.

Benzing, D. H., J. Seeman, and A. Renfrow (1978), The foliar epidermis in Tillandsioideae (Bromeliaceae) and its role in habitat selection, *Am. J. Bot.*, *65*, 359–365, doi:10.2307/2442278.

Borthagaray, A. I., M. E. Fuentes, and P. A. Marquet (2010), Vegetation pattern formation in a fog-dependent ecosystem, *J. Theor. Biol.*, *265*, 18–26, doi:10.1016/j.jtbi.2010.04.020.

Cereceda, P., H. Larrain, P. Osses, M. Farias, and I. Egana (2008a), The climate of the coast and fog zone in the Tarapaca Region, Atacama Desert, *Chile, Atmos. Res.*, *87*, 301–311, doi:10.1016/j.atmosres.2007.11.011.

Cereceda, P., H. Larrain, P. Osses, M. Farías, and I. Egaña (2008b), The spatial and temporal variability of fog and its relation to fog oases in the Atacama Desert, Chile, *Atmos. Res.*, *87*, 312–323, doi:10.1016/j.atmosres.2007.11.012.

Cerling, T. E. (1984), The stable isotopic composition of modern soil carbonate and its relationship to climate, *Earth Planet. Sci. Lett.*, *71*, 229–240, doi:10.1016/0012-821X(84)90089-X.

Dawson, T. E., S. Mambelli, A. H. Plamboeck, P. H. Templer, and K. P. Tu (2002), Stable isotopes in plant ecology, *Annu. Rev. Ecol. Syst.*, *33*, 507–559, doi:10.1146/annurev.ecolsys.33.020602.095451.

De Pol-Holz, R., O. Ulloa, F. Lamy, L. Dezileau, P. Sabatier, and D. Hebbeln (2007), Late Quaternary variability of sedimentary nitrogen isotopes in the eastern South Pacific Ocean, *Paleoceanography*, *22*, PA2207, doi:10.1029/2006PA001308.

Dietrich, W. E., and J. T. Perron (2006), The search for a topographic signature of life, *Nature*, *439*, 411–418, doi:10.1038/nature04452.

Ehleringer, J. R., P. W. Rundel, B. Palma, and H. A. Mooney (1998), Carbon isotope ratios of Atacama Desert plants reflect hyperaridity of region in northern Chile, *Rev. Chil. Hist. Nat.*, *71*, 79–86.

Ehleringer, J. R., D. R. Bowling, L. B. Flanagan, J. Fessenden, B. Helliker, L. A. Martinelli, and J. P. Ometto (2002), Stable isotopes and carbon cycle processes in forests and grasslands, *Plant Biol.*, *4*, 181–189, doi:10.1055/s-2002-25733.

Evans, R. D., and J. R. Ehleringer (1994), Plant $\delta^{15}N$ values along a fog gradient in the Atacama Desert, Chile, *J. Arid Environ.*, *28*, 189–193, doi:10.1016/S0140-1963(05)80056-4.

Franceschi, V. R., and P. A. Nakata (2005), Calcium oxalate in plants: Formation and function, Annu. *Rev. Plant Biol.*, *56*, 41–71, doi:10.1146/annurev.arplant.56.032604.144106.

Garreaud, R. D., and M. Falvey (2009), The coastal winds off western subtropical South America in future climate scenarios, *Int. J. Climatol.*, *29*, 543–554, doi:10.1002/joc.1716.

Garreaud, R. D., M. Vuille, and A. Clement (2003), The climate of the Altiplano: Observed current conditions and mechanisms of past changes, *Palaeogeogr. Palaeoclimatol. Palaeoecol.*, *194*, 5–22, doi:10.1016/S0031-0182(03)00269-4.

Garreaud, R., J. Barichivich, D. A. Christie, and A. Maldonado (2008), Interannual variability of the coastal fog at Fray Jorge relict forests in semi-arid Chile, *J. Geophys. Res.*, *113*, G04011, doi:10.1029/2008JG000709.

Garvie, L. A. J. (2003), Decay-induced biomineralization of the saguaro cactus (*Carnegiea gigantea*), *Am. Mineral.*, *88*, 1879–1888.

Garvie, L. A. J. (2006), Decay of cacti and carbon cycling, *Naturwissenschaften*, *93*, 114–118, doi:10.1007/s00114-005-0069-7.

Gonzalez, G., T. Dunai, D. Carrizo, and R. Allmendinger (2006), Young displacements on the Atacama Fault System, northern Chile from field observations and cosmogenic Ne-21 concentrations, *Tectonics*, *25*, TC3006, doi:10.1029/2005TC001846.

González, A. L., J. M. Fariña, R. Pinto, C. Pérez, K. C. Weathers, J. J. Armesto, and P. A. Marquet (2011), Bromeliad growth and stoichiometry: Responses to atmospheric nutrient inputs in fog-dependent ecosystems of the hyper-arid Atacama Desert, Chile, *Oecologia*, doi:10.1007/s00442-011-2032-y.

Graham, N. E., et al. (2007), Tropical Pacific: Mid-latitude teleconnections in medieval times, *Clim. Change*, *83*, 241–285, doi:10.1007/s10584-007-9239-2.

Handley, L. L., A. T. Austin, D. Robinson, C. M. Scrimgeour, J. A. Raven, T. H. E. Heaton, S. Schmidt, and G. R. Stewart (1999), The N-15 natural abundance (delta N-15) of ecosystem samples reflects measures of water availability, *Aust. J. Plant Physiol.*, *26*, 185–199, doi:10.1071/PP98146.

Houston, J. (2006), Variability of precipitation in the Atacama desert: Its causes and hydrological impact, *Int. J. Climatol.*, *26*, 2181–2198, doi:10.1002/joc.1359.

Javaux, E. J. (2006), Extreme life on Earth- past, present and possibly beyond, *Res. Microbiol.*, *157*, 37–48, doi:10.1016/j.resmic.2005.07.008.

Keeling, C. D. (1979), The Suess effect: ^{13}Carbon-^{14}carbon interrelations, *Environ. Int.*, *2*, 229–300, doi:10.1016/0160-4120(79)90005-9.

Lillywhite, H. B., and C. A. Navas (2006), Animals, energy, and water in extreme environments: Perspectives from Ithala 2004, *Physiol. Biochem. Zool.*, *79*, 265–273, doi:10.1086/499987.

Marquet, P. A., et al. (1998), Ecosystems of the Atacama Desert and adjacent Andean area in northern Chile, *Rev. Chil. Hist. Nat.*, *71*, 593–617.

Martin, C. E. (1994), Physiological ecology of the Bromeliaceae, *Bot. Rev.*, *60*, 1–82, doi:10.1007/BF02856593.

McCormac, F. G., A. G. Hogg, P. G. Blackwell, C. E. Buck, T. F. G. Higham, and P. J. Reimer (2004), SHCal04 Southern Hemisphere calibration, 0–11.0 cal kyr BP, *Radiocarbon*, *46*, 1087–1092.

McKay, C. P., E. I. Friedmann, B. Gomez-Silva, L. Caceres-Villanueva, D. T. Andersen, and R. Landheim (2003), Temperature and moisture conditions for life in the extreme arid region of the Atacama Desert: Four years of observations including the El Nino of 1997–1998, *Astrobiology*, *3*, 393–406, doi:10.1089/153110703769016460.

Moy, C. M., G. O. Seltzer, D. T. Rodbell, and D. M. Anderson (2002), Variability of El Niño/Southern Oscillation activity at millennial timescales during the Holocene epoch, *Nature*, *420*, 162–165, doi:10.1038/nature01194.

Peck, L. S., P. Convey, and D. K. A. Barnes (2006), Environmental constraints on life histories in Antarctic ecosystems: Tempos, timings and predictability, *Biol. Rev. Cambridge Philos. Soc.*, *81*, 75–109, doi:10.1017/S1464793105006871.

Pinto, R., I. Barria, and P. A. Marquet (2006), Geographical distribution of *Tillandsia* lomas in the Atacama Desert, northern Chile, *J. Arid Environ.*, *65*, 543–552, doi:10.1016/j.jaridenv.2005.08.015.

Proenca, S. L., and M. Das Gracas Sajo (2008), Anatomy of the floral scape of Bromeliaceae, *Rev. Bras. Bot.*, *31*, 399–408, doi:10.1590/S0100-84042008000300004.

Quade, J., J. A. Rech, C. Latorre, J. L. Betancourt, E. Gleeson, and M. T. K. Kalin (2007), Soils at the hyperarid margin: The isotopic composition of soil carbonate from the Atacama Desert, northern Chile, *Geochim. Cosmochim. Acta*, *71*, 3772–3795, doi:10.1016/j.gca.2007.02.016.

Rein, B., A. Luckge, and F. Sirocko (2004), A major Holocene ENSO anomaly during the Medieval period, *Geophys. Res. Lett.*, *31*, L17211, doi:10.1029/2004GL020161.

Rivera, E. R., and B. N. Smith (1979), Crystal morphology and ^{13}carbon/^{12}carbon composition of solid oxalate in cacti, *Plant Physiol.*, *64*, 966–970, doi:10.1104/pp.64.6.966.

Rundel, P. W., M. O. Dillon, B. Palma, H. A. Mooney, S. L. Gulmon, and J. R. Ehleringer (1991), The phytogeography and ecology of the Coastal Atacama and Peruvian Deserts, *Aliso*, *13*, 1–49.

Rundel, P. W., B. Palma, M. O. Dillon, M. R. Sharifi, E. T. Nilsen, and K. Boonpragob (1997), *Tillandsia landbeckii* in the coastal Atacama Desert of northern Chile, *Rev. Chil. Hist. Nat.*, *70*, 341–349.

SERNAGEOMIN (2003), *Mapa geológico de Chile: Versión digital*, *Publicación Geológica Digital (CD-ROM, versión1.0, 2003)*, Santiago, Chile.

Stuiver, M., and P. J. Reimer (1993), Extended ^{14}C database and revised CALIB radiocarbon calibration program, *Radiocarbon*, *35*, 215–230.

Stuiver, M., et al. (1998), INTCAL98 Radiocarbon age calibration 24,000 - 0 cal BP, *Radiocarbon*, *40*, 1041–1083.

Swap, R. J., J. N. Aranibar, P. R. Dowty, W. P. Gilhooly, and S. A. Macko (2004), Natural abundance of ^{13}C and ^{15}N in C_3 and C_4 vegetation of southern Africa: Patterns and implications, *Global Change Biol.*, *10*, 350–358, doi:10.1111/j.1365-2486.2003.00702.x.

Wang, L., P. D'Odorico, L. Ries, and S. A. Macko (2010), Patterns and implications of plant-soil δ13C and δ15N values in African savanna ecosystems, *Quat. Res.*, *73*, 77–83, doi:10.1016/j.yqres.2008.11.004.

Westbeld, A., O. Klemm, F. Griessbaum, E. Strater, H. Larrain, P. Osses, and P. Cereceda (2009), Fog deposition to a Tillandsia carpet in the Atacama Desert, *Ann. Geophys.*, *27*, 3571–3576, doi:10.5194/angeo-27-3571-2009.

J. M. Fariña, A. L. González, Claudio Latorre, Pablo A. Marquet, Pontificia Universidad Catolica de Chile, CASEB/Ecologia, Alameda 340, Santiago, 6513677, Chile.

R. Pinto, Dalmacia 3251, Iquique, Chile.

J. Quade, Department of Geosciences, University of Arizona, Tucson, AZ 85721, USA.